



RESEARCH LETTER

10.1002/2016GL071832

Key Points:

- GRACE suggests that more than 50% of total precipitation maybe missed by popular precipitation products in winter over the Tibetan plateau
- GRACE estimate agrees better with GPCP than other precipitation products, especially in cold months
- GRACE shows about 30% more annual precipitation than GPCP over the studied basins

Correspondence to:

A. Behrangi,
Ali.Behrangi@jpl.nasa.gov

Citation:

Behrangi, A., A. Gardner, J. T. Reager, and J. B. Fisher (2016), Using GRACE to constrain precipitation amount over cold mountainous basins, *Geophys. Res. Lett.*, 44, doi:10.1002/2016GL071832.

Received 3 NOV 2016

Accepted 26 DEC 2016

Accepted article online 28 DEC 2016

Using GRACE to constrain precipitation amount over cold mountainous basins

Ali Behrangi¹ , Alex S. Gardner¹, John T. Reager¹ , and Joshua B. Fisher¹ 

¹Jet Propulsion Laboratory, California Institute of Technology, Pasadena, California, USA

Abstract Despite the importance for hydrology and climate-change studies, current quantitative knowledge on the amount and distribution of precipitation in mountainous and high-elevation regions is limited due to instrumental and retrieval shortcomings. Here by focusing on two large endorheic basins in High Mountain Asia, we show that satellite gravimetry (Gravity Recovery and Climate Experiment (GRACE)) can be used to provide an independent estimate of monthly accumulated precipitation using mass balance equation. Results showed that the GRACE-based precipitation estimate has the highest agreement with most of the commonly used precipitation products in summer, but it deviates from them in cold months, when the other products are expected to have larger errors. It was found that most of the products capture about or less than 50% of the total precipitation estimated using GRACE in winter. Overall, Global Precipitation Climatology Project (GPCP) showed better agreement with GRACE estimate than other products. Yet on average GRACE showed ~30% more annual precipitation than GPCP in the study basins. In basins of appropriate size with an absence of dense ground measurements, as is a typical case in cold mountainous regions, we find GRACE can be a viable alternative to constrain monthly and seasonal precipitation estimates from other remotely sensed precipitation products that show large bias.

1. Introduction

Mountains and high-elevation regions can substantially impact regional weather and climate, and circulation of the global atmosphere. The interaction of mountainous topography and atmospheric circulation shapes the distribution of precipitation and significantly impacts water resources in many parts of the world [Renwick, 2014]. Projected tropospheric warming is expected to profoundly impact high-elevation temperatures, mountain glacier mass and distributions [Immerzeel et al., 2010; Marzeion et al., 2014; Radić et al., 2014], runoff regimes [Huss et al., 2010], and ecosystem functioning [Beniston, 2003]. To quantify and understand such impacts and processes, accurate quantification of precipitation is often fundamental but absent. High-relief and high-elevation regions typically have steep gradients in precipitation amounts. As such, accurate quantification requires dense in situ gauging networks and/or robust retrieval from satellite observations, but ground stations are typically sparse due to limited access and resources. In addition, in situ instrumentation often does not work well, or at all, in subzero temperatures. For example, in the Tibetan Plateau, the automatic gauge network is often switched off between October and March [Shen et al., 2010]. Functional gauges may also be largely biased, affected by several factors such as wind-induced undercatch [Goodison et al., 1998; Yang et al., 2005], while correction scaling factors can be 2 or greater during the snow season [Fuchs et al., 2001]. The lack of reliable ground measurements can also severely impact the performance of remotely sensed products as several studies have shown that bias correction of these products with ground data is needed and can significantly improve product skill [Yong et al., 2010; Tian et al., 2010; Krakauer et al., 2013; Gao and Liu, 2013; Behrangi et al., 2011, 2014a]. This is especially important in cold and mountainous regions where snow and mixed-phase precipitation are frequent but can be missed due to several factors such as insufficient sensitivity of sensors to capture precipitation signals, poor understanding of precipitation microphysics, and unknown surface emissivities [Ferraro et al., 2013]. Orographic precipitation enhancement [Shige et al., 2013] and difficulties in distinguishing between light rain and cloud [Berg et al., 2006; Lebsock and L'Ecuyer, 2011] and precipitation phases [Liu, 2008] are among additional challenges. Behrangi et al. [2014a, 2016] used CloudSat [Stephens et al., 2008], offering high sensitivity to retrieve light rain and snowfall, to calculate multiannual precipitation amount and distribution in high latitudes and utilized the results to assess several precipitation products. However, CloudSat temporal resolution and coverage limit its application for monthly and seasonal quantification of precipitation. Because of all of these issues, knowledge of the amount and

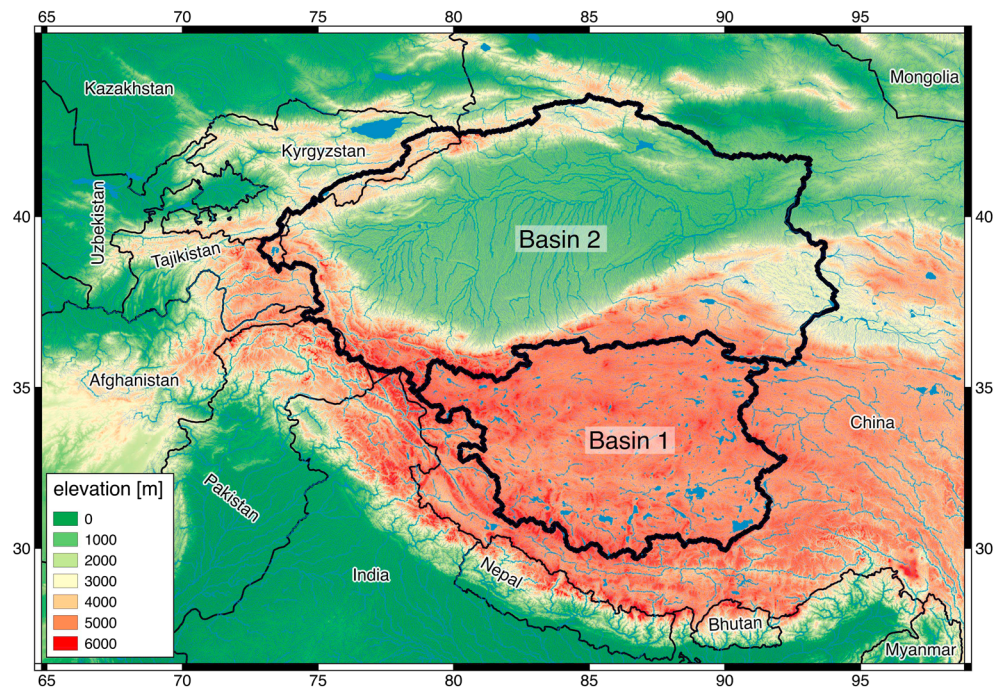


Figure 1. Location of the studied basins plotted over a colormap of surface elevations (GTOPO30) with river networks (HydroSHEDS v0) and lakes (HydroLAKES v1) shown in blue. Political boundaries are shown with thin black lines. Basin 1 and Basin 2 were defined as discrete collections of closed (not reaching ocean) HydroSHEDS v0 topographically defined hydrological basins.

distribution of precipitation in mountainous and high-elevation regions is generally poor [e.g., Behrangi et al., 2014b].

Here we show that the Gravity Recovery and Climate Experiment (GRACE) can be a useful alternative to estimate monthly precipitation in high-elevation regions. GRACE is a twin satellite mission measuring range rate variations between the two satellites by utilizing microwave interferometry and has been operational since 2002. Changes in gravity due to mass redistribution, such as water, within the Earth System perturb the GRACE orbit. Orbit perturbations are recorded as changes in range rates that can then be used to invert for the surface mass variations with high accuracy [Tapley et al., 2004]. Over land the hydrologic cycle causes time-varying gravity changes, so, by combining GRACE total water storage estimates with independent data, near-surface terrestrial water stores (e.g., snow, glaciers, and soil moisture) and groundwater have been investigated [e.g., Swenson and Wahr, 2007; Niu et al., 2007; Swenson et al., 2008; Landerer et al., 2010; Gardner et al., 2013]. While GRACE has been used to estimate precipitation amount in high latitudes [Swenson, 2010; Seo et al., 2010; Boening et al., 2012; Behrangi et al., 2016], its application for estimating precipitation in cold mountainous basins has not been explored. Furthermore, recent advancements in GRACE data processing have led to the development of more accurate “mascon” solutions, with lower uncertainty and less bias due to leakage effects [e.g., Watkins et al., 2015]. These solutions are well suited to serve as a precise constraint on mass changes over the mascon footprints, which reflect the intrinsic resolution at which the GRACE measurements are most viable. Specifically, the mascons were designed to allow for application of a priori information to prevent striping in the solutions, resulting in mass flux solutions that are shown to suffer less from leakage errors than harmonic solutions, and do not necessitate empirical filters [Watkins et al., 2015].

Here we use the Jet Propulsion Laboratory (JPL) GRACE mascon solution [Watkins et al., 2015] to calculate monthly precipitation in two basins in High Mountain Asia (Figure 1) and compare to several commonly used precipitation products. Basin 1 covers 650,000 km² of the western Tibetan Plateau and represents the combination of several small endorheic basins. Basin 2 covers an area of 1.282×10⁶ km² and includes the massive Tarim basin north of the Plateau and several smaller endorheic basins that surround the Taklamakan Desert.

The distribution of precipitation near and over the Tibetan Plateau can be described by two dominant precipitation systems during cold and warm seasons. Cold season precipitation peaks during February and March in the western part of the domain and is associated with propagating west-to-east midlatitude frontal systems. Warm season precipitation increases in coverage from south to north from late spring through late summer, associated with the large-scale Indian monsoon and often intense precipitation. During winter, the westerly flow impinges along the high-altitude terrain to the west and northwest of Basin 2, which is on the leeward side of the mountains, and thus precipitation is much more suppressed in winter. The monsoonal precipitation system begins in May and significantly impacts Basin 1, especially during July and August when intense precipitation (e.g., greater than 60 mm/month) covers the southern half of the basin.

Precipitation estimated from GRACE has three main advantages over other estimates in cold mountainous regions: (i) estimates are from an independent technique (gravimetry versus radiometry), and there is no need for empirical parameterizations, ground-based calibration, consideration for orographic enhancement, or correction for gauge undercatch issues; (ii) other satellite and ground measurements both face the highest detection and retrieval uncertainty in the presence of light rain, snow, and mixed-phase precipitation [Behrangi *et al.*, 2012, 2014c], but this is not the case for GRACE; and (iii) it measures total accumulation so does not miss precipitation falling between two satellite overpasses.

2. Method and Data

After processing to account for solid earth, tectonic, and aliased signals, and to reduce noise, GRACE mascons provide spatially gridded estimates of Terrestrial Water Storage Anomaly (TWSA) globally [Watkins *et al.*, 2015]. Precipitation accumulation is calculated from GRACE TWSA and based on the mass conservation principle, dictating that any change in one component of the water balance must be compensated by the same amount collectively in the other components [e.g., Dingman, 2008]. For accumulation start-time (e.g., first day of a month) t_1 and accumulation end-time (e.g., last day of a month) t_2 for domain D , the water storage change between time t_1 and t_2 is calculated as:

$$\Delta S = \int_{t_1}^{t_2} P(t) dt - \int_{t_1}^{t_2} ET(t) dt - \int_{t_1}^{t_2} \text{Sub}(t) dt - \int_{t_1}^{t_2} Q_{\text{net}}(t) dt \quad (1)$$

Where ΔS is the change in storage (i.e., from GRACE) between time t_1 and t_2 and $P(t)$, $ET(t)$, $\text{Sub}(t)$, $Q_{\text{net}}(t)$ are the precipitation rate, evapotranspiration rate, sublimation rate, and net lateral flux rate (e.g., runoff) for domain D at time t , respectively.

We obtained the 1° scaled version of GRACE TWSA version 2 mascon data product from GRACE Tellus website (available at grace.jpl.nasa.gov), whose processing is described in detail in Landerer and Swenson [2012]. This version includes improvements in both background geophysical models and orbital parameterization and is based on the recent mascon solution of surface mass change described in Watkins *et al.* [2015] and is combined with land surface model a priori information on spatial variability to recover a 1° signal.

Monthly evapotranspiration (ET) was calculated by averaging three observational products: PT-JPL [Fisher *et al.*, 2008], KZ-MOD [Zhang *et al.*, 2010, 2015], and SEBS [Su, 2002]. These products represent a spectrum of major global remote sensing ET products available and have been extensively validated for similar basin types [Vinukollu *et al.*, 2011; McCabe *et al.*, 2016; Miralles *et al.*, 2016]. Because the products have varying parameterizations and assumptions, we adopt an ensemble approach in this study. The calculated uncertainties for the ET ensemble (standard deviation between products) are consistent with those identified by Peng *et al.* [2016] over the Tibetan Plateau. Note that Moderate Resolution Imaging Spectroradiometer ET (MOD16) [Mu *et al.*, 2011] was not used in this study as it showed large areas of missing data over the study region. We obtained sublimation from European Centre for Medium-Range Weather Forecasts (ECMWF) Interim Reanalysis (ERA-Interim) [Dee *et al.*, 2011]. It was found that ECMWF sublimation values are often very small (about 3% of total ET in average), fairly negligible compared to the other water balance components. By selection, the net lateral flux (Q_{net}) is negligible as the two selected basins (Figure 1) are endorheic, which by definition is a closed drainage system that retains water and allows no outflow to other external bodies of water. For other applications in gauged basins, Q_{net} can be calculated from measurements of streamflow at basin outlets. Here we determined endorheic basins using the HydroSHEDS global database of drainage basin boundaries and the Global Self-consistent Hierarchical High-resolution Shorelines to identify large basins that do not drain to the ocean.

To compare GRACE precipitation estimates with other commonly used precipitation products, monthly precipitation rates from the following products were calculated over the studied basins: The Global Precipitation Climatology Centre (GPCC), the Global Precipitation Climatology Project (GPCP), TRMM 3B42-RT, TRMM 3B42 V7, TRMM 3A25, and the Asian Precipitation-Highly Resolved Observational Data Integration Toward Evaluation of Water Resources (APHRODITE) [Yatagai *et al.*, 2012]. GPCC ingests data from various organizations, networks, and other resources through bilateral contacts and thus utilizes more gauges than other popular gridded gauge products [Schneider *et al.*, 2014]. GPCC Full Data Reanalysis version 7.0 at $1^\circ \times 1^\circ$ resolution is used in this study. Further details regarding data access and construction of gridded precipitation products are described in Becker *et al.* [2013] and Schneider *et al.* [2014]. GPCP is a popular merged product utilizing GPCC and remotely sensed precipitation over both land and ocean. GPCC data are adjusted in GPCP for gauge undercatch using climatological factors. Here we used the latest (V2.1) daily $1^\circ \times 1^\circ$ resolution GPCP product [Huffman *et al.*, 2001] as it offers a finer resolution than the monthly $2.5^\circ \times 2.5^\circ$ resolution GPCP V2.2 product [Adler *et al.*, 2003; Huffman *et al.*, 2009]. TRMM 3B42-RT utilizes various precipitation products from various microwave (MW) sensors collected within a 3 h time bracket, maps the MW precipitation data onto quarter-degree grids, and fills the remained gaps with infrared estimates calibrated by MW precipitation products [Huffman *et al.*, 2007]. As part of the process the Tropical Rainfall Measuring Mission (TRMM) microwave imager is used as a reference to intercalibrate other microwave sensors to enhance the overall consistency among various types of MW sensors. TRMM 3B42 V7 is a bias-adjusted product by scaling the 3 h TRMM 3B42-RT estimates to sum to a monthly estimate from monthly gauge data. Furthermore, TRMM 3B42 V7 uses the TRMM Combined Instrument (TCI) from TRMM 2B31 product [Haddad *et al.*, 1997] as intercalibration reference for other MW precipitation estimates. Both TRMM 3B42 products are produced at $0.25^\circ \times 0.25^\circ$ spatial resolution every 3 h. We also used TRMM 3A25 product which is based on TRMM precipitation radar and is expected to better resolve orographic precipitation [Shige *et al.*, 2013] and mitigate some of the issues related to surface emissivity. Furthermore, we used APHRODITE [Yatagai *et al.*, 2012] which is a gauge-based precipitation product from daily precipitation data sets with high-resolution grids ($0.25^\circ \times 0.25^\circ$ daily) for Asia and uses several regionally available stations. Finally, as described in section 3, two CloudSat precipitation products were also used in this study to enhance the analyses and interpretation of the findings. The CloudSat 2C-PRECIPCOLUMN product [Haynes *et al.*, 2009] (release 04) was used to calculate frequency of rainfall, snowfall, and mixed precipitation over the study basin (only “certain” precipitation flags were considered). The 2C-SNOW-PROFILE [Wood *et al.*, 2014] was also used to calculate multiannual monthly snowfall rate during winter when snow is dominant. CloudSat rain estimates were not used in this study because the product is currently provisional over land and has not been evaluated.

The present study was performed using 6 years of data (from 2003 to 2009), constrained by the availability of data from GRACE (since late 2002) and ET (up to 2009 at the time of the analyses). Furthermore, APHRODITE was only available to 2008.

3. Results and Discussion

Figure 2 shows time series of monthly precipitation frequency from CloudSat (Figure 2a) and monthly precipitation accumulation from several precipitation products (Figure 2b) over Basin 1 shown in Figure 1. This basin has an average elevation of 5013 m above sea level and shows a strong seasonal cycle in precipitation, largely affected by monsoon. Both precipitation frequency (Figure 2a) and amount (Figure 2b) typically peak in summer and reach their minimum in winter. Snowfall occurs across all months and is often the only contributor to the total precipitation in winter (Figure 2a). Figure 2b suggests that TRMM 3B42-RT is an outlier, as it produces almost twice precipitation rate as other products and often with large spikes in summer and autumn. This can be partly related to the abundance of high clouds in summer and spring [Li *et al.*, 2006] and snow and ice surfaces in cold months. Microwave precipitation products used in TRMM 3B42-RT often have missing data over snow- and ice-covered regions and uses infrared-based precipitation estimates to fill the gaps in such conditions [Huffman *et al.*, 2007]. Plotting the time series of infrared (from TRMM 3B41) and microwave (from TRMM 3B40) precipitation estimates (not shown here) confirms that most of the large spike are related to the infrared-based estimates. After bias correction, TRMM 3B42 V7 is similar to GPCP and GPCC because both products use GPCC to remove bias at monthly time scale. APHRODITE and GPCC also show similar estimates, likely because they ingest data collected by many of the same automatic weather stations. The radar-only product (TRMM 3A25) persistently underestimates monthly precipitation rates compared to

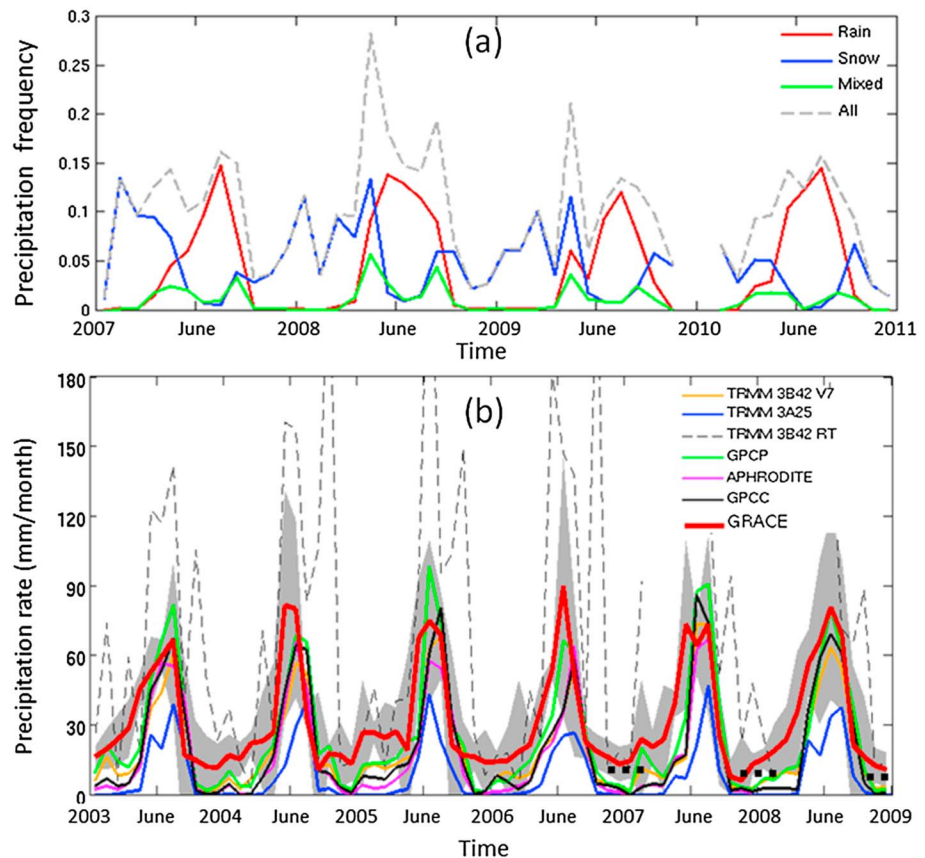


Figure 2. Precipitation analysis over Basin 1: (a) time series of monthly rainfall, snowfall, and mixed-phased precipitation frequency from CloudSat and (b) Comparison of monthly precipitation accumulation from several precipitation products. GRACE estimates in Figure 2a are shown in red color with gray shades representing 2σ uncertainties. The black dashed lines in Figure 2b represent winter mean snowfall rate from CloudSat. CloudSat data become available in late 2006.

the other products. TRMM radar has a minimum sensitivity of about 17 dBZ and thus can miss precipitation rates below about 0.5 mm h^{-1} , including light and moderate snowfall. Furthermore, ground clutter reflectivity at the lowest elevation scan, which over Basin 1 can be quite high and can coincide with the precipitating layer in the profile, might also contribute to the observed underestimation.

The GRACE-based precipitation estimate agrees well with other products (except TRMM 3A25 and TRMM 3B42-RT) during summer. However, it consistently shows higher monthly precipitation rates during cold months. Such a difference is consistent with our hypothesis, as the GRACE estimate is based on gravimetry and thus captures all types of precipitation, including light rain and snowfall that are dominant during cold months and can largely be missed by radar and gauge sensors [Behrangi et al., 2012, 2014c]. Furthermore, as shown in Behrangi et al. [2014c], microwave products can largely miss nonconvective precipitation systems that often form large fraction of total precipitation in cold months. Ground stations are also prone to instrumental failure and wind-induced undercatch during cold months [Goodison et al., 1998] that can result in that underestimation of precipitation compared to GRACE. Among the precipitation products shown in Figure 2b, GPCP was found closest to GRACE precipitation in most of months and closest to both GRACE and CloudSat during winter. Winter snowfall rate from CloudSat was calculated by averaging all snowfall rates (including zero) collected within the studied basins to enhance sampling size and thus stability of the estimates. Note that CloudSat is a polar low orbiter, crossing the equator at approximately at 1:30 A.M./P.M. and thus may not accurately represent the precipitation diurnal cycle. CloudSat estimates are not provided for other seasons as the CloudSat rain rate product is currently provisional over land and has not been evaluated.

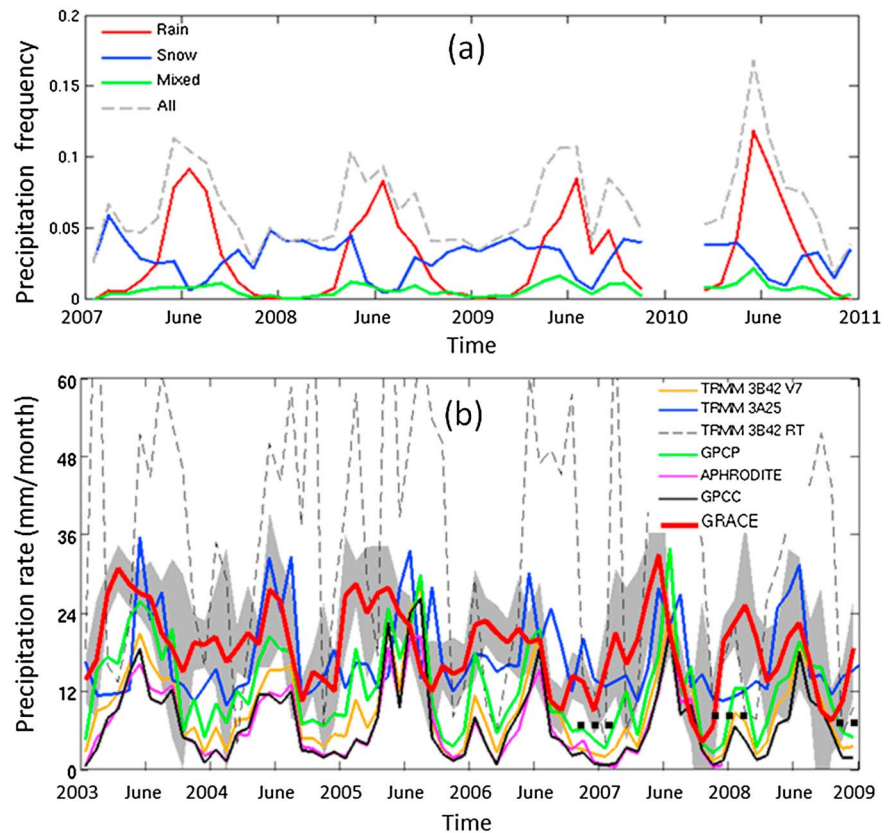


Figure 3. Similar to Figure 2 but for Basin 2.

A similar analysis was performed for Basin 2 that is located at lower elevation (2270 m on average) and higher latitude. This basin receives much less mean annual precipitation than Basin 1. Most of the precipitation in this basin occurs in summer. In winter precipitation mainly falls as snow. CloudSat suggests that snowfall can occur throughout the year including summer months (Figure 3a). The GRACE estimate shows similar seasonal precipitation patterns compared to the other products (Figure 3b), but in a few cases it displays large deviations. Similar to that observed in Basin 1, GRACE shows generally higher monthly accumulation during cold months. TRMM 3A25 shows the highest agreement with GRACE compared to the other products and is in contrast to the poor agreement observed for Basin 1. This might be related to the lower elevation of Basin 2 enabling radar to observe most of the precipitation profile, even after removing the lowest few bins affected by ground clutter. As shown in Figure 3b, the TRMM 3A25 estimate falls within 2σ uncertainty around GRACE estimate for most months. The GPCP estimate is the second closest estimate to GRACE followed by TRMM 3B42 V7. CloudSat mean snowfall rates in winter are also fairly consistent with GRACE and GPCP estimates and are larger than gauge products. Both GPCC and APHRODITE show almost no precipitation during the coldest months, presumably due to instrumental failure and the fact that several automatic gauges are switched off between October and March over Tibetan plateau [Shen *et al.*, 2010]. TRMM 3B42-RT seems to be an outlier as it estimates unrealistically high precipitation totals with large spikes, consistent with that observed in Basin 1.

Figure 4 summarizes the time series by comparing multiannual monthly precipitation from various precipitation products over Basin 1 (Figure 4a) and Basin 2 (Figure 4b). GRACE displays similar monthly precipitation accumulation patterns to the other precipitation products and shows that precipitation peaks around August while it reaches its minimum in December and January. The GRACE estimates agree closest to the other products in summer and are most distinct in winter. The closest estimate to GRACE is offered by GPCP in Basin 1 and TRMM 3A25, followed by GPCP, in Basin 2. Figure 4 suggests that from a GRACE perspective, existing precipitation products severely underestimate precipitation amount during cold months but are more consistent in summer months. This can be better observed by dividing the monthly precipitation estimate

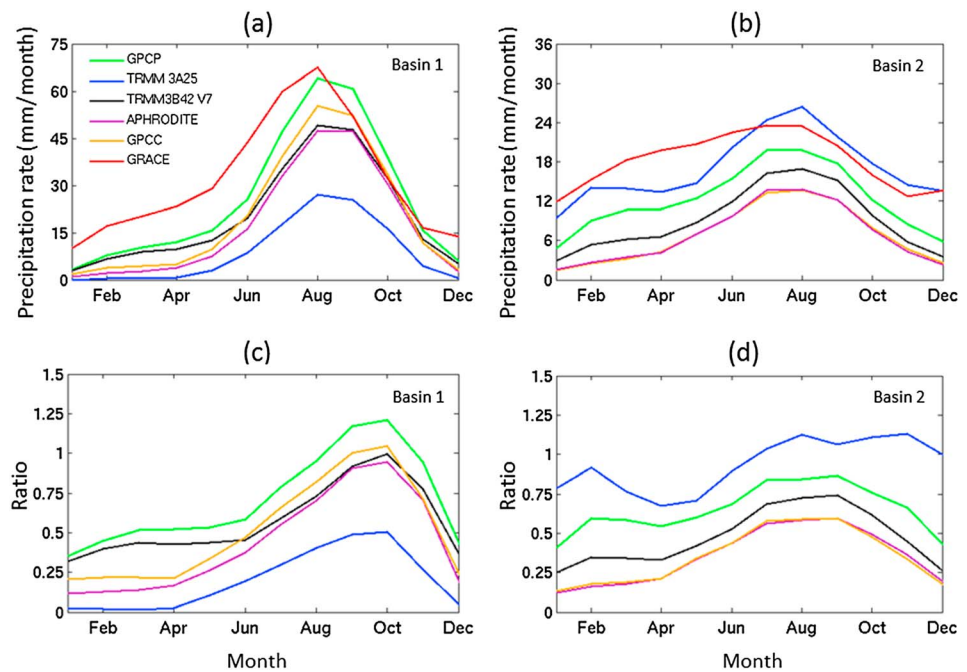


Figure 4. Multiannual monthly precipitation estimate from various precipitation products over (a) Basin 1 and (b) Basin 2. (c and d) Relative biases calculated by dividing monthly precipitation estimates of different products by that estimated from GRACE for Basins 1 and 2, respectively.

from different products by GRACE precipitation amounts, separately for Basin 1 (Figure 4c) and Basin 2 (Figure 4d). It can be seen that most of the products (except TRMM 3A25 in Basin 1) capture only 5%–60% of the GRACE estimate in winter. In warmer months, the products are more consistent with the GRACE estimate for Basin 1. For Basin 2 only GPCP and TRMM 3A25 agree (e.g., ratio between 0.75 and 1.25 as seen in Figure 4d) with GRACE, with the other products showing large underestimation (e.g., <75% of the GRACE estimate). Overall, GPCP showed better agreement with GRACE estimate of monthly precipitation amount than the other products. Even so, GRACE estimates gave 26% and 32% higher annual precipitation amounts when compared to GPCP for Basins 1 and 2, respectively.

4. Concluding Remarks

Current in situ and remotely sensed precipitation products often have low skill in estimating precipitation over cold mountainous regions. In this work Terrestrial Water Storage Anomaly observations from GRACE gravimetric measurements were used to constrain the water balance for total monthly precipitation for two endorheic basins in the western Tibetan Plateau and Taklamakan Desert. Remote sensing-based evapotranspiration was derived from an ensemble of products and their spread was used to estimate uncertainty in ET. Results showed that the GRACE-based precipitation estimate has the highest agreement with most of the products in summer but deviates greatly in cold months, when the other products are expected to have largest error and to undersample precipitation. It was found that most of the products (except TRMM 3A25 in Basin 1) capture only 10–60% of the total winter precipitation estimated by GRACE. Agreement between products in warmer months is found to be better. Overall, GPCP showed the best agreement (30% underestimation) with the GRACE estimate when compared to the other products.

There are several reasons to support the value of GRACE as an alternative for monthly precipitation estimation over high-elevation regions: (i) it provides an independent estimate using gravimetry (versus radiometry) method without a need for empirical parameterizations, ground calibration, consideration for orographic enhancement, atmospheric contamination, and correction for gauge undercatch issues; (ii) while satellite and ground stations face the highest detection and retrieval uncertainty during cold months, GRACE is not impacted; and (iii) GRACE-based estimates provide accumulated precipitation and thus differs from typical precipitation products that may miss precipitation falling between satellite overpasses. While satellite-based

ET retrievals are also limited during the coldest periods, ET happens to be relatively negligible during these times (as well as sublimation); hence, the water balance equation is tightly constrained by GRACE. Therefore, in the lack of sparse and high quality ground measurements, which is a typical case in cold mountainous regions, GRACE can be a viable alternative to constrain monthly or seasonal precipitation estimates from other remotely sensed precipitation products that tend to show significant biases. Nonetheless, our application succeeded in these regions in part due to the basins being endorheic; in other types of basins, lateral flow would need to be accounted for. Operationally, this approach is also limited to large basins, as the GRACE spatial resolution is relatively coarse. Overall, our study demonstrates that there is great potential for this approach to provide alternative estimate of precipitation amount in cold basins. The planned launch and operation of the GRACE Follow-on mission (gracefo.jpl.nasa.gov) in 2017 will ensure continuation of GRACE measurements for several more years.

Acknowledgments

We thank Terry Kubar of UCLA for discussion about meteorology of the study area. Data sets used in this study were collected from various sources: The latest version of daily GPCP (V2.1) from Goddard Earth Sciences Data and Information Services Center (GES DISC), GPCP Full Data Reanalysis version 7.0 at $1^\circ \times 1^\circ$ resolution from ftp://ftp.dwd.de/pub/data/gpcc/html/download_gate.html, GRACE total water storage from <http://grace.jpl.nasa.gov>, TRMM products from GES DISC, APHRODITE from the APHRODITE project <http://www.chi-kyu.ac.jp/precip/>, and CloudSat products are obtained from CloudSat data processing center: <http://www.cloudsat.cira.colostate.edu/data-products>. The research described in this paper was carried out at the Jet Propulsion Laboratory, California Institute of Technology, under a contract with the National Aeronautics and Space Administration. Financial support was also made available from NASA GRACE and GRACE-FO (NNH15ZDA001N-GRACE) and NASA Energy and Water Cycle Study (NNH13ZDA001N-NEWS) awards. Government sponsorship is acknowledged.

References

- Adler, R. F., et al. (2003), The version-2 Global Precipitation Climatology Project (GPCP) monthly precipitation analysis (1979–present), *J. Hydrometeorol.*, *4*(6), 1147–1167.
- Becker, A., P. Finger, A. Meyer-Christoffer, B. Rudolf, K. Schamm, U. Schneider, and M. Ziese (2013), A description of the global land-surface precipitation data products of the Global Precipitation Climatology Centre with sample applications including centennial (trend) analysis from 1901–present, *Earth Syst. Sci. Data*, *5*(1), 71–99.
- Behrangi, A., B. Khakbaz, T. C. Jaw, A. AghaKouchak, K. Hsu, and S. Sorooshian (2011), Hydrologic evaluation of satellite precipitation products over a mid-size basin, *J. Hydrol.*, *397*(3–4), 225–237.
- Behrangi, A., M. Lebsack, S. Wong, and B. Lambriksen (2012), On the quantification of oceanic rainfall using spaceborne sensors, *J. Geophys. Res.*, *117*, D20105, doi:10.1029/2012JD017979.
- Behrangi, A., G. Stephens, R. F. Adler, G. J. Huffman, B. Lambriksen, and M. Lebsack (2014a), An update on the oceanic precipitation rate and its zonal distribution in light of advanced observations from space, *J. Clim.*, *27*(11), 3957–3965.
- Behrangi, A., K. Andreadis, J. B. Fisher, F. J. Turk, S. Granger, T. Painter, and N. Das (2014b), Satellite-based precipitation estimation and its application for streamflow prediction over mountainous Western U.S. Basins, *J. Appl. Meteorol. Climatol.*, *53*(12), 2823–2842.
- Behrangi, A., Y. Tian, B. H. Lambriksen, and G. L. Stephens (2014c), What does CloudSat reveal about global land precipitation detection by other spaceborne sensors?, *Water Resour. Res.*, *50*, 4893–4905, doi:10.1002/2013WR014566.
- Behrangi, A., et al. (2016), Status of high-latitude precipitation estimates from observations and reanalyses, *J. Geophys. Res. Atmos.*, *121*, 4468–4486, doi:10.1002/2015JD024546.
- Beniston, M. (2003), Climatic change in mountain regions: A review of possible impacts, in *Climate Variability and Change in High Elevation Regions: Past, Present and Future*, edited by H. F. Diaz, pp. 5–31, Springer, Dordrecht, Netherlands.
- Berg, W., T. L'Ecuyer, and C. Kummerow (2006), Rainfall climate regimes: The relationship of regional TRMM rainfall biases to the environment, *J. Appl. Meteorol. Climatol.*, *45*(3), 434–454.
- Boening, C., M. Lebsack, F. Landerer, and G. Stephens (2012), Snowfall-driven mass change on the East Antarctic ice sheet, *Geophys. Res. Lett.*, *39*, L21501, doi:10.1029/2012GL053316.
- Dee, D. P., et al. (2011), The ERA-Interim reanalysis: Configuration and performance of the data assimilation system, *Q. J. R. Meteorol. Soc.*, *137*(656), 553–597.
- Dingman, S. L. (2008), *Physical Hydrology*, 2nd ed., 646 pp., Waveland Press, Long Grove, Ill.
- Ferraro, R. R., et al. (2013), An evaluation of microwave land surface emissivities over the continental United States to benefit GPM-Era precipitation algorithms, *IEEE Trans. Geosci. Remote Sens.*, *51*(1), 378–398.
- Fisher, J. B., K. P. Tu, and D. D. Baldocchi (2008), Global estimates of the land-atmosphere water flux based on monthly AVHRR and ISLSCP-II data, validated at 16 FLUXNET sites, *Remote Sens. Environ.*, *112*(3), 901–919.
- Fuchs, T., J. Rapp, F. Rubel, and B. Rudolf (2001), Correction of synoptic precipitation observations due to systematic measuring errors with special regard to precipitation phases, *Phys. Chem. Earth, Part B*, *26*(9), 689–693.
- Gao, Y. C., and M. F. Liu (2013), Evaluation of high-resolution satellite precipitation products using rain gauge observations over the Tibetan Plateau, *Hydrol. Earth Syst. Sci. Discuss.*, *9*(8), 9503–9532.
- Gardner, A. S., et al. (2013), A reconciled estimate of glacier contributions to sea level rise: 2003 to 2009, *Science*, *340*(6134), 852–857, doi:10.1126/science.1234532.
- Goodison, B. E., P. Y. T. Louie, and D. Yang (1998), *WMO Solid Precipitation Measurement Intercomparison*, vol. 67, 212 pp., World Meteorological Organization, Geneva.
- Haddad, Z. S., E. A. Smith, C. D. Kummerow, T. Iguchi, M. R. Farrar, S. L. Durden, M. Alves, and W. S. Olson (1997), The TRMM 'day-1' radar/radiometer combined rain-profiling algorithm, *J. Meteorol. Soc. Jpn.*, *75*(4), 799–809.
- Haynes, J. M., T. S. L'Ecuyer, G. L. Stephens, S. D. Miller, C. Mitrescu, N. B. Wood, and S. Tanelli (2009), Rainfall retrieval over the ocean with spaceborne W-band radar, *J. Geophys. Res.*, *114*, D00A22, doi:10.1029/2008JD009973.
- Huffman, G. J., R. F. Adler, M. M. Morrissey, D. T. Bolvin, S. Curtis, R. Joyce, B. McGavock, and J. Susskind (2001), Global precipitation at one-degree daily resolution from multisatellite observations, *J. Hydrometeorol.*, *2*(1), 36–50.
- Huffman, G. J., R. F. Adler, D. T. Bolvin, G. J. Gu, E. J. Nelkin, K. P. Bowman, Y. Hong, E. F. Stocker, and D. B. Wolff (2007), The TRMM multisatellite precipitation analysis (TMPA): Quasi-global, multiyear, combined-sensor precipitation estimates at fine scales, *J. Hydrometeorol.*, *8*(1), 38–55.
- Huffman, G. J., R. F. Adler, D. T. Bolvin, and G. Gu (2009), Improving the global precipitation record: GPCP Version 2.1, *Geophys. Res. Lett.*, *36*, L17808, doi:10.1029/2009GL040000.
- Huss, M., G. Jouviet, D. Farinotti, and A. Bauder (2010), Future high-mountain hydrology: A new parameterization of glacier retreat, *Hydrol. Earth Syst. Sci.*, *14*(5), 815–829.
- Immerzeel, W. W., L. P. H. van Beek, and M. F. P. Bierkens (2010), Climate change will affect the Asian water towers, *Science*, *328*(5984), 1382–1385.
- Krakauer, N., S. Pradhanang, T. Lakhankar, and A. Jha (2013), Evaluating satellite products for precipitation estimation in mountain regions: A case study for Nepal, *Remote Sens.*, *5*(8), 4107–4123.

- Landerer, F. W., and S. C. Swenson (2012), Accuracy of scaled GRACE terrestrial water storage estimates, *Water Resour. Res.*, *48*, W04531, doi:10.1029/2011WR011453.
- Landerer, F. W., J. O. Dickey, and A. Güntner (2010), Terrestrial water budget of the Eurasian pan-Arctic from GRACE satellite measurements during 2003–2009, *J. Geophys. Res.*, *115*, D23115, doi:10.1029/2010JD014584.
- Lebsock, M. D., and T. S. L'Ecuyer (2011), The retrieval of warm rain from CloudSat, *J. Geophys. Res.*, *116*, D20209, doi:10.1029/2011JD016076.
- Li, Y., X. Liu, and B. C. L. Chen (2006), Cloud type climatology over the Tibetan Plateau: A comparison of ISCCP and MODIS/TERRA measurements with surface observations, *Geophys. Res. Lett.*, *33*, L17716, doi:10.1029/2006GL026890.
- Liu, G. (2008), Deriving snow cloud characteristics from CloudSat observations, *J. Geophys. Res.*, *113*, D00A09, doi:10.1029/2007JD009766.
- Marzeion, B., J. G. Cogley, K. Richter, and D. Parkes (2014), Attribution of global glacier mass loss to anthropogenic and natural causes, *Science*, *345*(6199), 919–921, doi:10.1126/science.1254702.
- McCabe, M. F., A. Ershadi, C. Jimenez, D. G. Miralles, D. Michel, and E. F. Wood (2016), The GEWEX LandFlux project: Evaluation of model evaporation using tower-based and globally gridded forcing data, *Geosci. Model Dev.*, *9*(1), 283–305.
- Miralles, D., C. Jiménez, M. Jung, D. Michel, A. Ershadi, M. McCabe, M. Hirschi, B. Martens, A. Dolman, and J. Fisher (2016), The WACMOS-ET project—Part 2: Evaluation of global terrestrial evaporation data sets, *Hydrol. Earth Syst. Sci.*, *20*(2), 823–842.
- Mu, Q., M. Zhao, and S. W. Running (2011), Improvements to a MODIS global terrestrial evapotranspiration algorithm, *Remote Sens. Environ.*, *115*(8), 1781–1800.
- Niu, G.-Y., K.-W. Seo, Z.-L. Yang, C. Wilson, H. Su, J. Chen, and M. Rodell (2007), Retrieving snow mass from GRACE terrestrial water storage change with a land surface model, *Geophys. Res. Lett.*, *34*, L15704, doi:10.1029/2007GL030413.
- Peng, J., A. Loew, X. Chen, Y. Ma, and Z. Su (2016), Comparison of satellite-based evapotranspiration estimates over the Tibetan Plateau, *Hydrol. Earth Syst. Sci.*, *20*(8), 3167–3182.
- Radić, V., A. Bliss, A. C. Beedlow, R. Hock, E. Miles, and J. G. Cogley (2014), Regional and global projections of twenty-first century glacier mass changes in response to climate scenarios from global climate models, *Clim. Dyn.*, *42*(1–2), 37–58, doi:10.1007/s00382-013-1719-7.
- Renwick, J. (2014), MOUNTerrain: GEWEX Mountainous Terrain Precipitation Project, GEWEX news, vol. 24 No. 4, November 2014. [Available at http://www.gewex.org/gewex-content/files_mf/1432213914Nov2014.pdf]
- Schneider, U., A. Becker, P. Finger, A. Meyer-Christoffer, M. Ziese, and B. Rudolf (2014), GPCC's new land surface precipitation climatology based on quality-controlled in situ data and its role in quantifying the global water cycle, *Theor. Appl. Climatol.*, *115*(1–2), 15–40.
- Seo, K.-W., D. Ryu, B.-M. Kim, D. E. Waliser, B. Tian, and J. Eom (2010), GRACE and AMSR-E-based estimates of winter season solid precipitation accumulation in the Arctic drainage region, *J. Geophys. Res.*, *115*, D20117, doi:10.1029/2009JD013504.
- Shen, Y., A. Xiong, Y. Wang, and P. C. D. Xie (2010), Performance of high-resolution satellite precipitation products over China, *J. Geophys. Res.*, *115*, D02114, doi:10.1029/2009JD012097.
- Shige, S., S. Kida, H. Ashiwake, T. Kubota, and K. Aonashi (2013), Improvement of TMI Rain Retrievals in Mountainous Areas, *J. Appl. Meteorol. Climatol.*, *52*(1), 242–254.
- Stephens, G. L., et al. (2008), CloudSat mission: Performance and early science after the first year of operation, *J. Geophys. Res.*, *113*, D00A18, doi:10.1029/2008JD009982.
- Su, Z. (2002), The Surface Energy Balance System (SEBS) for estimation of turbulent heat fluxes, *Hydrol. Earth Syst. Sci.*, *6*, 85–99.
- Swenson, S. (2010), Assessing high-latitude winter precipitation from global precipitation analyses using GRACE, *J. Hydrometeorol.*, *11*(2), 405–420.
- Swenson, S., and J. Wahr (2007), Multi-sensor analysis of water storage variations of the Caspian Sea, *Geophys. Res. Lett.*, *34*, L16401, doi:10.1029/2007GL030733.
- Swenson, S., J. Famiglietti, J. Basara, and J. C. W. Wahr (2008), Estimating profile soil moisture and groundwater variations using GRACE and Oklahoma Mesonet soil moisture data, *Water Resour. Res.*, *44*, W01413, doi:10.1029/2007WR006057.
- Tapley, B. D., S. Bettadpur, J. C. Ries, P. F. Thompson, and M. M. Watkins (2004), GRACE measurements of mass variability in the Earth system, *Science*, *305*(5683), 503–505.
- Tian, Y., C. D. Peters-Lidard, and J. B. Eylander (2010), Real-time bias reduction for satellite-based precipitation estimates, *J. Hydrometeorol.*, *11*(6), 1275–1285.
- Vinukollu, R. K., E. F. Wood, C. R. Ferguson, and J. B. Fisher (2011), Global estimates of evapotranspiration for climate studies using multi-sensor remote sensing data: Evaluation of three process-based approaches, *Remote Sens. Environ.*, *115*, 801–823.
- Watkins, M. M., D. N. Wiese, D.-N. Yuan, C. Boening, and F. W. C. J. B. Landerer (2015), Improved methods for observing Earth's time variable mass distribution with GRACE using spherical cap mascons, *J. Geophys. Res. Solid Earth*, *120*, 2648–2671, doi:10.1002/2014JB011547.
- Wood, N. B., T. S. L'Ecuyer, A. J. Heymsfield, G. L. Stephens, D. R. Hudak, and P. Rodriguez (2014), Estimating snow microphysical properties using collocated multisensor observations, *J. Geophys. Res. Atmos.*, *119*, 8941–8961.
- Yang, D., D. Kane, Z. Zhang, D. Legates, and B. Goodison (2005), Bias corrections of long-term (1973–2004) daily precipitation data over the northern regions, *Geophys. Res. Lett.*, *32*, L19501, doi:10.1029/2005GL024057.
- Yatagai, A., K. Kamiguchi, O. Arakawa, A. Hamada, N. Yasutomi, and A. Kito (2012), APHRODITE: Constructing a long-term daily gridded precipitation dataset for Asia based on a dense network of rain gauges, *Bull. Am. Meteorol. Soc.*, *93*(9), 1401–1415.
- Yong, B., L.-L. Ren, Y. Hong, J.-H. Wang, J. J. Gourley, S.-H. Jiang, X. Chen, and W. C. W. Wang (2010), Hydrologic evaluation of Multisatellite Precipitation Analysis standard precipitation products in basins beyond its inclined latitude band: A case study in Laohahe basin, China, *Water Resour. Res.*, *46*, W07542, doi:10.1029/2009WR008965.
- Zhang, K., J. S. Kimball, R. R. Nemani, and S. W. C. W. Running (2010), A continuous satellite-derived global record of land surface evapotranspiration from 1983 to 2006, *Water Resour. Res.*, *46*(9), 1–21, doi:10.1029/2009WR008800.
- Zhang, K., J. S. Kimball, R. R. Nemani, S. W. Running, Y. Hong, J. J. Gourley, and Z. Yu (2015), Vegetation greening and climate change promote multidecadal rises of global land evapotranspiration, *Sci. Rep.*, *5*, 15956.